Journal of Applied and Computational Mechanics, Vol. 3, No. 1, (2017), 60-79
DOI: 10.22055/jacm.2017.12620

Shahid Chamran University

Journal of
Applied and Computational Mechanics

Thermo-mechanical nonlinear vibration analysis of fluid-conveying structures subjected to different boundary conditions using Galerkin-Newton-Harmonic balancing method

M. G. Sobamowo[1], B. Y. Ogunmola[2], C. A. Osheku[3]

[1, 2] Department of Mechanical Engineering, University of Lagos, Akoka, Lagos, Nigeria.
[3] Centre for Space Transport and Propulsion, National Space Research and Development Agency, Federal Ministry of Science and Technology, FCT, Abuja, Nigeria.

Received January 09 2017; revised January 25 2017; accepted for publication February 12 2017.
Corresponding author: M. G. Sobamowo, mikegbeminiyi@gmail.com

Abstract

The development of mathematical models for describing the dynamic behaviours of fluid conveying pipes, micro-pipes and nanotubes under the influence of some thermo-mechanical parameters results into nonlinear equations that are very difficult to solve analytically. In cases where the exact analytical solutions are presented either in implicit or explicit forms, high skills and rigorous mathematical analyses were employed. It is noted that such solutions do not provide general exact solutions. Inevitably, comparatively simple, flexible yet accurate and practicable solutions are required for the analyses of these structures. Therefore, in this study, approximate analytical solutions are provided to the nonlinear equations arising in flow-induced vibration of pipes, micro-pipes and nanotubes using Galerkin-Newton-Harmonic Method (GNHM). The developed approximate analytical solutions are shown to be valid for both small and large amplitude oscillations. The accuracies and explicitness of these solutions were examined in limiting cases to establish the suitability of the method.

Keywords: Thermo-mechanical; Non-linear Vibration; Galerkin's method; Newton-Harmonic Balancing Technique; Fluid-conveying structure.

1. Introduction

Nonlinear flow-induced vibration of pipes, micro-pipes and nanotube has been the topic of experimental, numerical, and theoretical studies as it has attracted a large number of studies in literatures [1-37]. This is because, modeling the dynamic behaviours of the structures under the influence of some thermo-fluidic or thermo-mechanical parameters often results in nonlinear equations and such are difficult to find the exact analytical solutions. In some cases where decomposition procedures into spatial and temporal parts are carried out, the resulting nonlinear equation for the temporal part comes in form of Duffing equation. Application of analytical methods such as Exp-function method, He's Exp-function method, improved F-expansion method, Lindstedt-Poincare techniques, quotient trigonometric function expansion method to the nonlinear equation present analytical solutions either in implicit or explicit form which often involved complex mathematical analysis leading to analytic expression involving a large number terms. Furthermore, the methods are time-consuming task accompanied with possessing high skills in mathematics. Also, they do not provide general analytical solutions since the solutions often come with conditional statements (i.e. except in limited circumstances where exact analytical solutions are possible) which make them limited in used as many of the conditions with the exact solutions do not meet up with the practical applications since they give approximated solutions that hardly provide an all-encompassing understanding of the nature of systems in response to parameters affecting nonlinearity. Also, in practice, analytical solutions with large number of terms and conditional statements for the solutions are not convenient for use by designers and engineers [38]. Consequently, recourse has always been made to numerical methods or approximate analytical methods in solving the problems [39-61]. However, the classical way for finding exact analytical solution is obviously still very important since it serves as an accurate benchmark for numerical solutions. Also, the experimental data are useful to access the mathematical models, but are never sufficient to verify the numerical solutions of the established mathematical models. Comparison between the numerical calculations and experimental data often fail to reveal the compensation of modelling deficiencies through the computational errors or unconscious approximations in establishing applicable numerical schemes. Additionally, exact analytical solutions for specified problems are also essential for the development of efficient applied numerical simulation tools. Inevitably, exact analytical expressions are required to show the direct relationship between the models parameters. When such exact analytical solutions are available, they provide good insights into the significance of various system parameters affecting the phenomena as it gives continuous physical insights than pure numerical or computation methods. Furthermore, most of the analytical approximation and purely numerical methods that were applied in literatures to nonlinear problems are computationally intensive. Exact analytical expression is more convenient for engineering calculations compare with experimental or numerical studies and it serves as a starting point for a better understanding of the relationship between physical quantities/properties. It is convenient for parametric studies, accounting for the physics of the problem and appears more appealing than the numerical solutions. It appears more appealing than the numerical solution as it helps to reduce the computation costs, simulations and task in the analysis of real life problems. Therefore, an exact analytical solution is required for the problem. Newton-Hamonic Balancing technique as proposed by Lai *et al.* [62] is a comparatively new technique for nonlinear cubic-quintic Duffing equation. The simplicity, flexibility in application, and avoidance of complicated numerical integration has given the approach added advantages over the previous methods. Combining the Galerkin's method with Newton-Hamonic Balancing technique in the analysis of non-linear initial-boundary value problems, provides complementary advantages of higher accuracy, reduced computation cost and task as compared to the other methods as found in literature. Therefore, in this research, analytical solutions are provided to the nonlinear partial differential equations arising in flow-induced vibration in pipes, micro-pipes and nanotubes under different boundary conditions using Galerkin-Newton-Hamonic Balancing Method. The nonlinear partial differential equations were converted to nonlinear ordinary differential equations and then Newton-Hamonic Balancing technique is utilized to provide exact analytical solutions to the nonlinear ordinary differential equations of vibration of the structures. The developed analytical solutions are compared with the numerical results and the results of approximate analytical solutions and good agreements reached. The analytical solutions can serve as a starting point for a better understanding of the relationship between the physical quantities of the problems as it provides continuous physical insights into the problem than pure numerical or computation methods.

2. Governing equations and boundary conditions

Case 1: Flow-induced vibration in pipe

Consider a pipe conveying hot fluid, subjected to stretching effects and resting on linear and nonlinear elastic foundation (Pasternak, linear and nonlinear Winkler foundation) under external applied tension and global pressure as shown in Fig. 1. Using nonlocal elasticity theory and Hamilton's principle, we arrived at the governing equation of motion as:

$$\begin{aligned} &EI\frac{\partial^4 w}{\partial x^4}+(m_p+m_f)\frac{\partial^2 w}{\partial t^2}+\mu\frac{\partial w}{\partial t}+2vm_f\frac{\partial^2 w}{\partial x\,\partial t}+\left(m_f v^2+PA-T-k_p-\frac{EA\alpha\Delta\theta}{1-2\nu}\right)\frac{\partial^2 w}{\partial x^2} \\ &+k_1 w+k_3 w^3-\left[N_o+\frac{EA}{2L}\int_0^L\left(\frac{\partial w}{\partial x}\right)^2 dx\right]\frac{\partial^2 w}{\partial x^2}=0 \end{aligned} \tag{1}$$

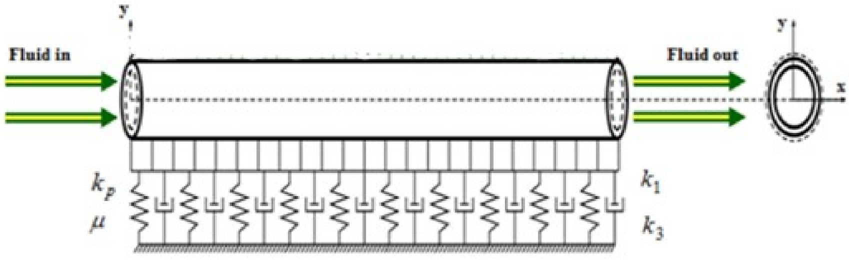

Fig. 1. Pipe conveying hot fluid

If the pipe is slightly curved, then the governing equation becomes

$$EI\frac{\partial^4 w}{\partial x^4}+(m_p+m_f)\frac{\partial^2 w}{\partial t^2}+\mu\frac{\partial w}{\partial t}+2vm_f\frac{\partial^2 w}{\partial x\partial t}+\left(m_f v^2+PA-T-k_p-\frac{EA\alpha\Delta\theta}{1-2v}\right)\frac{\partial^2 w}{\partial x^2}$$
$$+k_1 w+k_3 w^3-\left[N_o+\frac{EA}{2L}\int_0^L\left\{\frac{\partial Z_o}{\partial x}\frac{\partial w}{\partial x}+\left(\frac{\partial w}{\partial x}\right)^2\right\}dx\right]\left[\frac{\partial^2 w}{\partial x^2}+\frac{\partial^2 Z_o}{\partial x^2}\right]=0 \tag{2}$$

Where $Z_o(x)$ is the arbitrary initial rise function. Using the Galerkin's decomposition procedure to separate the spatial and temporal parts of the lateral displacement functions as

$$w(x,t)=\phi(x)u(t) \tag{3}$$

Where $u(t)$ the generalized coordinate of the system and $\phi(x)$ is a trial/comparison function that will satisfy both the geometric and natural boundary conditions. Applying one-parameter Galerkin's solution given in Eq. (4) to Eq. (3):

$$\int_0^L R(x,t)\phi(x)dx \tag{4-a}$$

where for the straight pipe:

$$R(x,t)=EI\frac{\partial^4 w}{\partial x^4}+(m_p+m_f)\frac{\partial^2 w}{\partial t^2}+\mu\frac{\partial w}{\partial t}+2vm_f\frac{\partial^2 w}{\partial x\partial t}+\left(m_f v^2+PA-T-k_p-\frac{EA\alpha\Delta\theta}{1-2v}\right)\frac{\partial^2 w}{\partial x^2}$$
$$+k_1 w+k_3 w^3-\left[N_o+\frac{EA}{2L}\int_0^L\left(\frac{\partial w}{\partial x}\right)^2 dx\right]\frac{\partial^2 w}{\partial x^2}=0 \tag{4-b}$$

And for the slightly curved pipe:

$$R(x,t)=EI\frac{\partial^4 w}{\partial x^4}+(m_p+m_f)\frac{\partial^2 w}{\partial t^2}+\mu\frac{\partial w}{\partial t}+2vm_f\frac{\partial^2 w}{\partial x\partial t}+\left(m_f v^2+PA-T-k_p-\frac{EA\alpha\Delta\theta}{1-2v}\right)\frac{\partial^2 w}{\partial x^2}$$
$$+k_1 w+k_3 w^3-\left[N_o+\frac{EA}{2L}\int_0^L\left\{\frac{\partial Z_o}{\partial x}\frac{\partial w}{\partial x}+\left(\frac{\partial w}{\partial x}\right)^2\right\}dx\right]\left[\frac{\partial^2 w}{\partial x^2}+\frac{\partial^2 Z_o}{\partial x^2}\right]=0 \tag{4-c}$$

We have the nonlinear vibration equation of the pipe as:

$$M\ddot{u}(t)+G\dot{u}(t)+(K+C)u(t)-Vu^3(t)=0 \tag{5}$$

where

$$M=\int_0^L (m_p+m_f)\phi^2(x)dx$$
$$G=\int_0^L\left[2m_f u\phi(x)\left(\frac{d\phi}{dx}\right)+\mu\phi^2(x)\right]dx$$
$$K=\int_0^L\left[EI\phi(x)\frac{d^4\phi}{dx^4}+k_1\phi^2(x)+k_p\phi(x)\frac{d^2\phi}{dx^2}\right]dx$$
$$C=\int_0^L\left(m_f u^2+PA-T-\frac{EA\alpha\Delta\theta}{1-2v}\right)\phi(x)\frac{d^2\phi}{dx^2}dx$$
$$V=\int_0^L\left\{\phi(x)\left[N_o+\frac{EA}{2L}\int_0^L\left(\frac{\partial w}{\partial x}\right)^2 dx\right]\frac{d^2\phi}{dx^2}-k_3\phi^3(x)\right\}dx$$

For the slightly curved pipe, M, G, K and C are the same but:

$$V=\int_0^L\left\{\phi(x)\left[N_o+\frac{EA}{2L}\int_0^L\left\{\frac{\partial Z_o}{\partial x}\frac{\partial w}{\partial x}+\left(\frac{\partial w}{\partial x}\right)^2\right\}dx\right]\left[\frac{\partial^2 w}{\partial x^2}+\frac{\partial^2 Z_o}{\partial x^2}\right]-k_3\phi^3(x)\right\}dx \tag{6-a}$$

The circular fundamental natural frequency gives

$$\omega_n=\sqrt{\frac{K+C^*}{M}} \tag{6-b}$$

where

$$C^*=\int_0^L\left(PA-T-\frac{EA\alpha\Delta\theta}{1-2v}\right)\phi(x)\frac{d^2\phi}{dx^2}dx \tag{6-c}$$

Case 2: Flow induced vibration in functionally graded micro-pipe

Consider the case of flow induced vibration in a functionally graded micropipe conveying hot fluid subjected to stretching effects and resting on linear and nonlinear elastic foundation under external applied tension and global pressure. Applying strain gradient and coupled stress theories followed by Hamilton's principle [28], we arrived at the governing equation of motion for the functionally graded micropipe given as:

$$\left[GA_{eq}\left(2l_o^2+\frac{4}{5}l_1^2\right)\right]\frac{\partial^6 w}{\partial x^6}+\left[EI+GA_{eq}\left(2l_o^2+\frac{8}{15}l_1+l_1^2\right)\right]\frac{\partial^4 w}{\partial x^4}+(m_p+m_f)\frac{\partial^2 w}{\partial t^2}+\mu\frac{\partial w}{\partial t}+2vm_f\frac{\partial^2 w}{\partial x\,\partial t}$$
$$+\left(m_f v^2+PA-T-k_p-\frac{EA\alpha\Delta\theta}{1-2\nu}\right)\frac{\partial^2 w}{\partial x^2}+k_1 w+k_3 w^3-\left[N_o+\frac{EA}{2L}\int_0^L\left(\frac{\partial w}{\partial x}\right)^2 dx\right]\frac{\partial^2 w}{\partial x^2}=0 \tag{7}$$

If the pipe is slightly curved, then the governing equation for the FG micropipe becomes:

$$\left[GI_{eq}\left(2l_o^2+\frac{4}{5}l_1^2\right)\right]\frac{\partial^6 w}{\partial x^6}+\left[EI_{eq}+GA_{eq}\left(2l_o^2+\frac{8}{15}l_1+l_1^2\right)\right]\frac{\partial^4 w}{\partial x^4}+(m_p+m_f)\frac{\partial^2 w}{\partial t^2}+\mu\frac{\partial w}{\partial t}+2vm_f\frac{\partial^2 w}{\partial x\,\partial t}$$
$$+\left(m_f v^2+PA-T-k_p-\frac{EA_{eq}\alpha\Delta\theta}{1-2\nu}\right)\frac{\partial^2 w}{\partial x^2}+k_1 w+k_3 w^3-\left[N_o+\frac{EA_{eq}}{2L}\int_0^L\left\{\frac{\partial Z_o}{\partial x}\frac{\partial w}{\partial x}+\left(\frac{\partial w}{\partial x}\right)^2\right\}dx\right]\left[\frac{\partial^2 w}{\partial x^2}+\frac{\partial^2 Z_o}{\partial x^2}\right]=0 \tag{8}$$

where

$$EI_{eq}=\int_A E(r)z^2 dA=\int_0^{2\pi}\int_{r_i}^{r_o}E(r)r^2 sin^2(\theta)(rdrd\theta)$$

$$GI_{eq}=\int_A G(r)z^2 dA=\int_0^{2\pi}\int_{r_i}^{r_o}EG(r)r^2 sin^2(\theta)(rdrd\theta)$$

$$EA_{eq}=\int_A E(r)dA=\int_0^{2\pi}\int_{r_i}^{r_o}E(r)(rdrd\theta)$$

$$GA_{eq}=\int_A G(r)dA=\int_0^{2\pi}\int_{r_i}^{r_o}G(r)(rdrd\theta)$$

$$E(r)=\left(\frac{r_o-r}{r_o-r_i}\right)^n E^i+\left[1-\left(\frac{r_o-r}{r_o-r_i}\right)^n\right]E^o$$

$$\mathrm{G}(r)=\left(\frac{r_o-r}{r_o-r_i}\right)^n G^i+\left[1-\left(\frac{r_o-r}{r_o-r_i}\right)^n\right]G^o$$

$$\alpha(r)=\left(\frac{r_o-r}{r_o-r_i}\right)^n \alpha^i+\left[1-\left(\frac{r_o-r}{r_o-r_i}\right)^n\right]\alpha^o$$

$$m_p=\rho A$$

$$\rho(r)=\left(\frac{r_o-r}{r_o-r_i}\right)^n \rho^i+\left[1-\left(\frac{r_o-r}{r_o-r_i}\right)^n\right]\rho^o$$

in which l_o, l_1 and l_2 are the independent length scale parameters embedded in the constitutive equations of the higher order stresses. If we follow the same procedure of applying the Galerkin's decomposition procedure to separate the spatial and temporal parts of the lateral displacement and then apply the one-parameter Galerkin's solution, we arrived at the same nonlinear vibration equation for the micropipe as:

$$M\ddot{u}(t)+G\dot{u}(t)+(K+C)u(t)-Vu^3(t)=0 \tag{9}$$

But at this time, we have

$$M=\int_0^L (m_p+m_f)\phi^2(x)dx$$

$$G=\int_0^L\left[2m_f u\phi(x)\left(\frac{d\phi}{dx}\right)+\mu\phi^2(x)\right]dx$$

$$K=\int_0^L\left\{\left[EI+GA_{eq}\left(2l_o^2+\frac{8}{15}l_1+l_1^2\right)\right]\phi(x)\frac{d^4\phi}{dx^4}+\left[GA_{eq}\left(2l_o^2+\frac{4}{5}l_1^2\right)\right]\frac{\partial^6\phi}{\partial x^6}+k_1\phi^2(x)+k_p\phi(x)\frac{d^2\phi}{dx^2}\right\}dx$$

$$C=\int_0^L\left(m_f u^2+PA-T-\frac{EA\alpha\Delta\theta}{1-2\nu}\right)\phi(x)\frac{d^2\phi}{dx^2}dx$$

$$V=\int_0^L\phi(x)\left\{\left[N_o+\frac{EA}{2L}\int_0^L\left(\frac{\partial\phi}{\partial x}\right)^2 dx\right]\frac{d^2\phi}{dx^2}-k_3\frac{d^3\phi}{dx^3}\right\}dx$$

For the slightly curved FG micropipe, *M, G, K* and *C* are the same but

$$V=\int_0^L \phi(x)\left\{\left[N_o+\frac{EA}{2L}\int_0^L\left\{\frac{\partial Z_o}{\partial x}\frac{\partial w}{\partial x}+\left(\frac{\partial w}{\partial x}\right)^2\right\}dx\right]\left[\frac{\partial^2 w}{\partial x^2}+\frac{\partial^2 Z_o}{\partial x^2}\right]-k_3\frac{d^3\phi}{dx^3}\right\}dx$$

The circular fundamental natural frequency gives:

$$\omega_n=\sqrt{\frac{K+C^*}{M}} \tag{10}$$

where

$$C^*=\int_0^L\left(PA-T-\frac{EA\alpha\Delta\theta}{1-2\nu}\right)\phi(x)\frac{d^2\phi}{dx^2}dx$$

Case 3: Flow-induced vibration in nanotube

Consider a single-walled carbon nanotube conveying hot fluid, subjected to stretching effects and resting on linear and nonlinear elastic foundation under external applied tension and global pressure. Following the Eringen's nonlocal elasticity theory [63-66] and Hamilton's principle, we arrived at the governing equation of motion for the single-walled carbon nanotube (SWCBT) as:

$$\begin{aligned}&EI\frac{\partial^4 w}{\partial x^4}+(m_p+m_f)\frac{\partial^2 w}{\partial t^2}+\mu\frac{\partial w}{\partial t}+2\nu m_f\frac{\partial^2 w}{\partial x\partial t}+\left(m_f\nu^2+PA-T-k_p-\frac{EA\alpha\Delta\theta}{1-2\nu}\right)\frac{\partial^2 w}{\partial x^2}-\left[\frac{EA}{2L}\int_0^L\left(\frac{\partial w}{\partial x}\right)^2dx\right]\frac{\partial^2 w}{\partial x^2}\\&+k_1w+k_3w^3-(e_oa)^2\left[\begin{aligned}&(m_p+m_f)\frac{\partial^4 w}{\partial x^2\partial t^2}+\mu\frac{\partial^3 w}{\partial x^2\partial t}+k_1\frac{\partial^2 w}{\partial x^2}+6k_3w\left(\frac{\partial w}{\partial x}\right)^2+3w^2\frac{\partial w}{\partial x}+2\nu m_f\frac{\partial^4 w}{\partial x^3\partial t}\\&+\left(m_f\nu^2+PA-T-k_p-\frac{EA\alpha\Delta\theta}{1-2\nu}\right)\frac{\partial^4 w}{\partial x^4}-\left[\frac{EA}{2L}\int_0^L\left(\frac{\partial w}{\partial x}\right)^2dx\right]\frac{\partial^4 w}{\partial x^4}\end{aligned}\right]=0\end{aligned} \tag{11}$$

If the nanotube is slightly curved, then the governing equation for the nanotube becomes:

$$\begin{aligned}&EI\frac{\partial^4 w}{\partial x^4}+(m_p+m_f)\frac{\partial^2 w}{\partial t^2}+\mu\frac{\partial w}{\partial t}+2\nu m_f\frac{\partial^2 w}{\partial x\partial t}+\left(m_f\nu^2+PA-T-k_p-\frac{EA\alpha\Delta\theta}{1-2\nu}\right)\frac{\partial^2 w}{\partial x^2}\\&-\left[N_o+\frac{EA}{2L}\int_0^L\left\{\frac{\partial Z_o}{\partial x}\frac{\partial w}{\partial x}+\left(\frac{\partial w}{\partial x}\right)^2\right\}dx\right]\left[\frac{\partial^2 w}{\partial x^2}+\frac{\partial^2 Z_o}{\partial x^2}\right]+k_1w+k_3w^3\\&-(e_oa)^2\left[\begin{aligned}&(m_p+m_f)\frac{\partial^4 w}{\partial x^2\partial t^2}+\mu\frac{\partial^3 w}{\partial x^2\partial t}+k_1\frac{\partial^2 w}{\partial x^2}+6k_3w\left(\frac{\partial w}{\partial x}\right)^2+3w^2\frac{\partial w}{\partial x}+2\nu m_f\frac{\partial^4 w}{\partial x^3\partial t}\\&+\left(m_f\nu^2+PA-T-k_p-\frac{EA\alpha\Delta\theta}{1-2\nu}\right)\frac{\partial^4 w}{\partial x^4}-\left[N_o+\frac{EA}{2L}\int_0^L\left\{\frac{\partial Z_o}{\partial x}\frac{\partial w}{\partial x}+\left(\frac{\partial w}{\partial x}\right)^2\right\}dx\right]\left[\frac{\partial^4 w}{\partial x^4}+\frac{\partial^4 Z_o}{\partial x^4}\right]\end{aligned}\right]=0\end{aligned} \tag{12}$$

For nanotube conveying fluid, the radius of the tube is assumed to be the characteristics length scale, Knudsen number is larger than 10^{-2}. Therefore, the assumption of no-slip boundary conditions does not hold and modified model should be used. Therefore, we have:

$$VCF=\frac{U_{avg,slip}}{U_{avg,no-slip}}=\left(1+a_kKn\right)\left[4\left(\frac{2-\sigma_v}{\sigma_v}\right)\left(\frac{Kn}{1+Kn}\right)+1\right] \tag{13}$$

where Kn is the Knudsen number, σ_v is tangential moment accommodation coefficient which is considered to be 0.7 for most practical purposes [67].

$$a_k=a_o\frac{2}{\pi}\left[tan^{-1}\left(a_1Kn^B\right)\right] \tag{14}$$

$$a_o=\frac{64}{3\pi\left(1-\frac{4}{b}\right)} \tag{15}$$

Therefore,

$$U_{avg,slip}=\left(1+a_kKn\right)\left[4\left(\frac{2-\sigma_v}{\sigma_v}\right)\left(\frac{Kn}{1+Kn}\right)+1\right]U_{avg,no-slip}=VCF\left(U_{avg,no-slip}\right) \tag{16}$$

and Eq. (12) could be written as

$$\begin{gathered}EI\frac{\partial^4 w}{\partial x^4}+(m_p+m_f)\frac{\partial^2 w}{\partial t^2}+\mu\frac{\partial w}{\partial t}+2m_f\left[VCF\left(U_{avg,no-slip}\right)\right]\frac{\partial^2 w}{\partial x\partial t}+\left(m_f\left[VCF\left(U_{avg,no-slip}\right)\right]^2+PA-T-k_p-\frac{EA\alpha\Delta\theta}{1-2\nu}\right)\frac{\partial^2 w}{\partial x^2}\\-\left[N_o+\frac{EA}{2L}\int_0^L\left\{\frac{\partial Z_o}{\partial x}\frac{\partial w}{\partial x}+\left(\frac{\partial w}{\partial x}\right)^2\right\}dx\right]\left[\frac{\partial^2 w}{\partial x^2}+\frac{\partial^2 Z_o}{\partial x^2}\right]+k_1w+k_3w^3\\-(e_oa)^2\left[\begin{gathered}(m_p+m_f)\frac{\partial^4 w}{\partial x^2\partial t^2}+\mu\frac{\partial^3 w}{\partial x^2\partial t}+k_1\frac{\partial^2 w}{\partial x^2}+6k_3w\left(\frac{\partial w}{\partial x}\right)^2+3w^2\frac{\partial w}{\partial x}+2m_f\left[VCF\left(U_{avg,no-slip}\right)\right]\frac{\partial^4 w}{\partial x^3\partial t}\\+\left(m_f\left[VCF\left(U_{avg,no-slip}\right)\right]^2+PA-T-k_p-\frac{EA\alpha\Delta\theta}{1-2\nu}\right)\frac{\partial^4 w}{\partial x^4}-\left[N_o+\frac{EA}{2L}\int_0^L\left\{\frac{\partial Z_o}{\partial x}\frac{\partial w}{\partial x}+\left(\frac{\partial w}{\partial x}\right)^2\right\}dx\right]\left[\frac{\partial^4 w}{\partial x^4}+\frac{\partial^4 Z_o}{\partial x^4}\right]\end{gathered}\right]=0\end{gathered}\tag{17}$$

Again, following the same procedural method, the Galerkin's decomposition procedure and then apply the one-parameter Galerkin's solution, we arrived at the same nonlinear vibration equation for the nanotube as:

$$M\ddot{u}(t)+G\dot{u}(t)+(K+C)u(t)-Vu^3(t)=0\tag{18}$$

Here, we have

$$M=\int_0^L(m_p+m_f)\phi(x)\left(\phi(x)-(e_oa)^2\frac{d^2\phi}{dx^2}\right)+\phi(x)\left(m_fu^2\phi(x)-(e_oa)^2\frac{d^2\phi}{dx^2}\right)dx$$

$$G=\int_0^L\phi(x)\left\{\left(2m_fv\frac{d\phi}{dx}-(e_oa)^2\frac{d^3\phi}{dx^3}\right)+\left(\mu\phi(x)-(e_oa)^2\frac{d^2\phi}{dx^2}\right)\right\}dx$$

$$K=\int_0^L\phi(x)\left\{EI\frac{d^4\phi}{dx^4}+k_1\phi(x)-k_p\frac{d^2\phi}{dx^2}-k_1\left(e_oa\right)^2\frac{d^2\phi}{dx^2}+\left(e_oa\right)^2k_p\frac{d^2\phi}{dx^2}\right\}dx$$

$$C=\int_0^L\left(m_fu^2+PA-T-\frac{EA\alpha\Delta\theta}{1-2\nu}\right)\phi(x)\left(\frac{d^2\phi}{dx^2}-(e_oa)^2\frac{d^4\phi}{dx^4}\right)dx$$

$$V=\int_0^L\phi(x)\left\{\begin{gathered}\left[N_o+\frac{EA}{2L}\int_0^L\left(\frac{\partial\phi}{\partial x}\right)^2dx\right]\frac{d^2\phi}{dx^2}-k_3\frac{d^3\phi}{dx^3}(x)+6k_3(e_oa)^2\phi(x)\left(\frac{\partial\phi}{\partial x}\right)^2\\-3k_3(e_oa)^2\phi^2(x)\frac{\partial\phi}{\partial x}-(e_oa)^2\left[N_o+\frac{EA}{2L}\int_0^L\left(\frac{\partial\phi}{\partial x}\right)^2dx\right]\frac{d^4\phi}{dx^4}\end{gathered}\right\}dx$$

For the slightly curved nanotube, *M, G, K* and *C* are the same but:

$$V=\int_0^L\phi(x)\left\{\begin{gathered}\left[N_o+\frac{EA}{2L}\int_0^L\left\{\frac{\partial Z_o}{\partial x}\frac{\partial w}{\partial x}+\left(\frac{\partial w}{\partial x}\right)^2\right\}dx\right]\left[\frac{\partial^2 w}{\partial x^2}+\frac{\partial^2 Z_o}{\partial x^2}\right]-k_3\frac{d^3\phi}{dx^3}(x)+6k_3(e_oa)^2\phi(x)\left(\frac{\partial\phi}{\partial x}\right)^2\\-3k_3(e_oa)^2\phi^2(x)\frac{\partial\phi}{\partial x}-(e_oa)^2\left[N_o+\frac{EA}{2L}\int_0^L\left\{\frac{\partial Z_o}{\partial x}\frac{\partial w}{\partial x}+\left(\frac{\partial w}{\partial x}\right)^2\right\}dx\right]\left[\frac{\partial^4 w}{\partial x^4}+\frac{\partial^4 Z_o}{\partial x^4}\right]\end{gathered}\right\}dx\tag{19-a}$$

and the circular fundamental natural frequency gives:

$$\omega_n=\sqrt{\frac{K+C^*}{M}}\tag{19-b}$$

where:

$$C^*=\int_0^L\left(PA-T-\frac{EA\alpha\Delta\theta}{1-2\nu}\right)\phi(x)\left(\frac{d^2\phi}{dx^2}-(e_oa)^2\frac{d^4\phi}{dx^4}\right)dx\tag{19-c}$$

3. The initial and boundary conditions

The structures (pipe, micro-pipe and nanotube) may be subjected to any of the following boundary conditions.

i. Clamped-Clamped (doubly clamped)

Where the trial/comparison function are given as:

$$\phi(x)=cosh\,\beta_nx-cos\,\beta_nx-\left(\frac{cosh\,\beta_nL-cos\,\beta_nL}{sinh\,\beta_nL-sin\,\beta_nL}\right)\left(sinh\,\beta_nx-sin\,\beta_nx\right)\tag{20}$$

or

$$\phi(x) = cosh\,\beta_n x - cos\,\beta_n x - \left(\frac{sinh\,\beta_n L + sin\,\beta_n L}{cosh\,\beta_n L - cos\,\beta_n L}\right)\left(sinh\,\beta_n x - sin\,\beta_n x\right) \tag{21}$$

where β_n are the roots of the equation $cos\,\beta_n L\, cosh\,\beta_n L = 1$. The initial and the boundary conditions are:

$$w(0,x) = A \;\; \dot{w}(0,x) = 0 \tag{22-a}$$

$$w(0,t) = w'(0,t) = 0 \;\; w(L,t) = w'(L,t) = 0 \tag{22-b}$$

The applications of space function as given above for clamped-clamped will involve long calculations and expressions in finding *M, G, K, C,* and *V*, alternatively, a polynomial function of the form Eq. (23) can be applied for this type of support system:

$$\phi(x) = a_o + a_1 X + a_2 X^2 + a_3 X^3 + a_4 X^4 \tag{23}$$

where $X = \frac{x}{L}$. Applying the boundary conditions

$$\phi(x) = \left(X^2 - 2X^3 + X^4\right)a_4 \tag{24}$$

Orthogonal function should satisfy the equation

$$\int_0^a \phi(X)\phi(X)dx = 1 \tag{25}$$

Substitute Eq. (24) into Eq. (25), we have

$$a_4 = 3\sqrt{70}\left(\sqrt{\frac{1}{a^5\left(70a^4 - 315a^3 + 540a^2 - 420a + 126\right)}}\right) \tag{26}$$

For a =1, arrived at $a_4 = 25.20$ for the first mode.

ii. Clamped-Simple supported

The trial/comparison function is given as:

$$\phi(x) = cosh\,\beta_n x - cos\,\beta_n x - \left(\frac{cosh\,\beta_n L - cos\,\beta_n L}{sinh\,\beta_n L - sin\,\beta_n L}\right)\left(sinh\,\beta_n x - sin\,\beta_n x\right) \tag{27}$$

where β_n are the roots of the equation, $tan\,\beta_n L = tanh\,\beta_n L$. The initial and the boundary conditions are:

$$w(0,x) = A \;\; \dot{w}(0,x) = 0 \tag{28-a}$$

$$w(0,t) = w'(0,t) = 0 \;\; w(L,t) = w''(L,t) = 0 \tag{28-b}$$

Alternatively, a polynomial function of the form Eq. (29) can be applied for this type of support system:

$$\phi(x) = \left(\frac{3}{2}X^2 - \frac{5}{2}X^3 + X^4\right)a_4 \tag{29}$$

on using orthogonal functions, $a_4 = 11.625$ for the first mode.

iii. Simple-Simple supported

$$\phi(x) = sin\,\beta_n x\,,\; sin\,\beta L = 0 \;\; \Rightarrow \beta_n = \frac{n\pi}{L} \tag{30}$$

The initial and the boundary conditions are:

$$w(0,x) = A \;\; \dot{w}(0,x) = 0 \tag{31-a}$$

$$w(0,t) = w''(0,t) = 0 \;\; w(L,t) = w''(L,t) = 0 \tag{31-b}$$

Alternatively, a polynomial function of the form Eq. (31) can be applied for this type of support system.

$$\phi(x) = \left(X - 2X^3 + X^4\right)a_4 \tag{32}$$

On using orthogonal functions, $a_4 = 3.20$ for the first mode

iv. Clamp-Free (cantilever)

$$\phi(x) = cosh\,\beta_n x - cos\,\beta_n x - \left(\frac{cosh\,\beta_n L + cos\,\beta_n L}{sinh\,\beta_n L + sin\,\beta_n L}\right)\left(sinh\,\beta_n x - sin\,\beta_n x\right) \tag{33}$$

or

$$\phi(x) = cosh\,\beta_n x - cos\,\beta_n x - \left(\frac{sinh\,\beta_n L - sin\,\beta_n L}{cosh\,\beta_n L - cos\,\beta_n L}\right)(sinh\,\beta_n x - sin\,\beta_n x) \tag{34}$$

β_n are the roots of the equation $cos\beta_n L cosh\beta_n L = -1$. The initial and the boundary conditions are:

$$w(0,x) = A \;\; \dot{w}(0,x) = 0 \tag{35-a}$$

$$w(0,t) = w'(0,t) = 0 \;\; w''(L,t) = w'''(L,t) = 0 \tag{35-b}$$

Alternatively, a polynomial function of the form Eq. (36) can be applied for this type of support system:

$$\phi(x) = \left(6X^2 - 4X^3 + X^4\right)a_4 \tag{36}$$

Also, with the aid of orthogonal functions, $a_4 = 0.6625$ for the first mode

4. Nonlinear natural frequency by Newton-balancing method

If we substitute $\tau = \omega t$, the nonlinear equation (18) to be solved can be written as

$$\omega^2 \ddot{u}(\tau) + \frac{(K+C)}{M}u(\tau) - \frac{V}{M}u^3(\tau) = 0 \tag{37}$$

Since for the undamped clamped-clamped, clamped-simple and simple-simple supported structures, *G = 0.* Applying Newton's procedure, the displacement and the squared angular frequency can be expressed as

$$u(\tau) = u_1(\tau) + \Delta u_1(\tau) \tag{38}$$

$$\omega^2 = \omega_1^2 + \Delta\omega_1^2 \tag{39}$$

Substituting Eq. (38) and (39) results into Eq. (37) gives

$$\left(\omega_1^2 + \Delta\omega_1^2\right)\left[\ddot{u}_1(\tau) + \Delta\ddot{u}_1(\tau)\right] + \frac{(K+C)}{M}\left[u_1(\tau) + \Delta u_1(\tau)\right] - \frac{V}{M}\left[u_1(\tau) + \Delta u_1(\tau)\right]^3 = 0 \tag{40}$$

On linearizing Eq. (40) with respect to the correction terms $\Delta u_1(\tau)$ and $\Delta\omega_1$, we have

$$\begin{aligned}&\left(\omega_1^2 + \Delta\omega_1^2\right)\ddot{u}_1(\tau) + \omega_1^2\Delta\ddot{u}_1(\tau) + \frac{(K+C)}{M}\left[u_1(\tau)\right] - \frac{V}{M}\left[u_1^3(\tau)\right] \\ &+ \frac{(K+C)}{M}\left[\Delta u_1(\tau)\right] - \frac{3V}{M}\left[u_1^2(\tau)\right]\left[\Delta u_1(\tau)\right] = 0\end{aligned} \tag{41}$$

In order to find the periodic solution of Eq. (38), assume an initial approximation to $u_1(\tau)$

$$u_1(\tau) = A\cos\tau \tag{42}$$

The above Eq. (42) is a periodic function of τ of period 2π. On substituting $u_1(\tau) = A\cos\tau$ into Eq. (41) gives:

$$\begin{aligned}&-\left(\omega_1^2 + \Delta\omega_1^2\right)A\cos\tau - \omega_1^2\Delta\ddot{u}_1 + \frac{(K+C)}{M}\left[A\cos\tau\right] - \frac{V}{M}\left[A^3\cos^3\tau\right] \\ &+ \frac{(K+C)}{M}\left[\Delta\left(A\cos\tau\right)\right] - \frac{3V}{M}\left[A^2\cos^2\tau\right]\left[\Delta\left(A\cos\tau\right)\right] = 0\end{aligned} \tag{43}$$

Eq.(42) can be expressed as:

$$-\left(\omega_1^2 + \Delta\omega_1^2\right)A\cos\tau + \omega_1^2\Delta\left(\ddot{u}_1(t)\right) + f\left(A\cos\tau\right) + f_x\left(A\cos\tau\right)\Delta u_1 = 0 \tag{44}$$

where Δu_1 is a periodic function of τ of period 2π. We have the following Fourier series expansion:

$$f\left(A\cos\tau\right) = \sum_{i=1}^{\infty} a_{2i-1}\cos\left[(2i-1)\tau\right] \tag{45}$$

$$f_x\left(A\cos\tau\right) = \frac{b_o}{2} + \sum_{i=1}^{\infty} b_{2i}\cos\left[(2i-1)\tau\right] \tag{46-a}$$

where the Fourier coefficients are:

$$a_1 = \frac{(K+C)A}{M} - \frac{3VA^3}{4M} \;\; a_3 = -\frac{VA^3}{4M} \;\; b_o = \frac{2(K+C)}{M} - \frac{3VA^2}{M} \;\; b_2 = -\frac{3VA^2}{2M} \tag{46-b}$$

4.1 First-order analytical approximation

For the first-order analytical approximation, we get:

$$\Delta u_1(\tau) = 0 \tag{47}$$

$$\Delta\omega_1^2 = 0 \tag{48}$$

and therefore

$$u(\tau) = u_1(\tau) = A\cos\tau \tag{49}$$

On substituting Eq. (45), (46), (47) and (48) into Eq. (44), expanding the resulting expression in a trigonometric series and then setting the coefficient of $cos\,\tau$ to zero results in the first-order analytical approximation ω_1. The corresponding approximate analytical periodic solution $u_1(\tau)$ can be expressed as:

$$u_1(\tau) = A\cos(\omega_1\tau) \tag{50}$$

in which

$$\omega_1 = \sqrt{\frac{K+C}{M} - \frac{3VA^2}{4M}} \tag{51}$$

where angular frequency ω_1 is the first-order analytical approximation. We can write Eq. (50) directly in terms of the primary parameters in the governing equations as:

$$u_1(\tau) = A\cos\left\{\left(\sqrt{\frac{K+C}{M} - \frac{3VA^2}{4M}}\right)\tau\right\} \tag{1}$$

4.2 Second-order analytical approximation

For the second-order analytical approximation, we set

$$\Delta u_1(\tau) = c_1\left[\cos(\tau) - \cos(3\tau)\right] \tag{53}$$

By substituting Eq. (45), (46) and (53) into Eq. (44), follow by a trigonometric series expansion and then setting the coefficients of $cos\,\tau$ and $cos\,3\tau$ to zero result in a set of simultaneous equation in terms of c_1 and $\Delta\omega_1^2$

$$2a_1 + b_o c_1 - b_4 c_1 - 2A\,\Delta\omega_1 - 2A\,\omega_1 - 2c_1\omega_1 = 0 \tag{54}$$

$$2a_3 - b_o c_1 + b_2 c_1 + 2c_1\omega_1 = 0 \tag{55}$$

Solving Eqs. (54) and (55) simultaneously, we have

$$\Delta\omega_1^2 = \frac{a_3\left(Ab_o - 2a_1\right)}{A\left[A\left(b_o - b_2\right) - 18a_1\right]} = \frac{3A^4\left(\frac{4V}{M}\right)^2}{128\left[16\left(\frac{K+C}{M}\right) + 12A^2\left(\frac{V}{M}\right)\right]} \tag{56}$$

$$c_1 = \frac{2Aa_3}{A\left(b_o - b_2\right) - 18a_1} = \frac{-A^3V}{8M\left[4\left(\frac{K+C}{M}\right) + 3A^2\left(\frac{V}{M}\right)\right]} \tag{57}$$

The corresponding approximate analytical periodic solution $u_2(\tau)$ is given as

$$u_2(\tau) = u_1(\tau) + \Delta u_1(\tau) = A\cos(\omega_2 t) + c_1\left[\cos(\omega_2 t) - \cos(3\omega_2 t)\right] \tag{58}$$

Recall from Eq. (39) that $\omega^2 = \omega_1^2 + \Delta\omega_1^2$. Therefore, the second-order analytical approximation frequency is given as:

$$\omega_2 = \sqrt{\omega_1^2 + \Delta\omega_1^2} \tag{59}$$

From Eqs. (51) and (56), we have

$$\omega_2 = \sqrt{\frac{128\left(\frac{K+C}{M}\right)^2 + 69A^4\left(\frac{V}{M}\right)^2 + 192A^2\left(\frac{K+C}{M}\right)\left(\frac{V}{M}\right)}{8\left[16\left(\frac{K+C}{M}\right) + 12A^2\left(\frac{V}{M}\right)\right]}} \tag{60}$$

We can re-write Eq. (58) directly in terms of the primary parameters in the governing equations by substituting Eqs. (57) and (59) into Eq. (58) to have

$$u_2(\tau)=A\cos\left(\left\{\sqrt{\frac{128\left(\frac{K+C}{M}\right)^2+69A^4\left(\frac{V}{M}\right)^2+192A^2\left(\frac{K+C}{M}\right)\left(\frac{V}{M}\right)}{8\left[16\left(\frac{K+C}{M}\right)+12A^2\left(\frac{V}{M}\right)\right]}}\right\}t\right)$$
$$-\left(\frac{A^3V}{8M\left[4\left(\frac{K+C}{M}\right)+3A^2\left(\frac{V}{M}\right)\right]}\right)\left[\begin{array}{l}\cos\left(3\left\{\sqrt{\frac{128\left(\frac{K+C}{M}\right)^2+69A^4\left(\frac{V}{M}\right)^2+192A^2\left(\frac{K+C}{M}\right)\left(\frac{V}{M}\right)}{8\left[16\left(\frac{K+C}{M}\right)+12A^2\left(\frac{V}{M}\right)\right]}}\right\}t\right)\\-\cos\left(\left\{\sqrt{\frac{128\left(\frac{K+C}{M}\right)^2+69A^4\left(\frac{V}{M}\right)^2+192A^2\left(\frac{K+C}{M}\right)\left(\frac{V}{M}\right)}{8\left[16\left(\frac{K+C}{M}\right)+12A^2\left(\frac{V}{M}\right)\right]}}\right\}t\right)\end{array}\right] \tag{61}$$

4.3 Third-order analytical approximation

For the third-order analytical approximation, the relevant expressions must be extended. Going back to Eqs.(38), (39) and (41), replacing $u_1(\tau)$, $\Delta u_1(\tau)$, ω_1 and $\Delta\omega_1$ by $u_2(\tau)$, $\Delta u_2(\tau)$, ω_2 and $\Delta\omega_2$, respectively, in the equations, we have:

$$\begin{aligned}&\left(\omega_2^2+\Delta\omega_2^2\right)\left[-A\cos\tau+c_1\left[9\cos(3\tau)-\cos(\tau)\right]\right]-\omega_2^2\Delta\ddot{u}_2(\tau)\\&+\frac{(K+C)}{M}\left[A\cos\tau+c_1\left[\cos(\tau)-\cos(3\tau)\right]\right]-\frac{V}{M}\left[A\cos\tau+c_1\left[\cos(\tau)-\cos(3\tau)\right]\right]^3\\&+\frac{(K+C)}{M}\left[\Delta\left[A\cos\tau+c_1\left[\cos(\tau)-\cos(3\tau)\right]\right]\right]-\frac{3V}{M}\left[A\cos\tau+c_1\left[\cos(\tau)-\cos(3\tau)\right]\right]^2=0\end{aligned} \tag{62}$$

As before, Eq. (61) can be expressed as:

$$\begin{aligned}&\left(\omega_2^2+\Delta\omega_2^2\right)\left[-A\cos\tau+c_1\left[9\cos(3\tau)-\cos(\tau)\right]\right]-\omega_2^2\Delta\left[-A\cos\tau+c_1\left[9\cos(3\tau)-\cos(\tau)\right]\right]\\&+f\left(A\cos\tau+c_1\left[\cos(\tau)-\cos(3\tau)\right]\right)+f_x\left(A\cos\tau+c_1\left[\cos(\tau)-\cos(3\tau)\right]\right)\Delta u_2=0\end{aligned} \tag{63}$$

For the third-order analytical approximation, we set:

$$\Delta u_2(\tau)=c_2\left[\cos(\tau)-\cos(3\tau)\right]+c_3\left[\cos(3\tau)-\cos(5\tau)\right] \tag{64}$$

Substitute Eq. (64) into Eq. (63), employing a trigonometric series expansion and then setting the coefficients of $\cos\tau$, $\cos 3\tau$ and $\cos 5\tau$ to zero yields a set of simultaneous equation in terms of c_2, c_3 and $\Delta\omega_2^2$ as given in Eq. (65-67):

$$\begin{aligned}&\frac{3(A+c_1)^3V}{2M}-\frac{3(A+c_1)^2Vc_1}{2M}-2\omega_2(A+c_1)+2\left(\frac{K+C}{M}\right)(A+c_1)+\frac{3(A+c_1)Vc_1^2}{M}\\&c_2\left[\frac{3(A+c_1)^2V}{M}+\frac{3(A+c_1)Vc_1}{M}+2\left(\frac{K+C}{M}\right)+\frac{3(A+c_1)Vc_1^2}{M}-2\omega_2^2\right]\\&c_3\left[\frac{3(A+c_1)^2V}{2M}-\frac{3Vc_1^2}{2M}-\frac{3(A+c_1)Vc_1}{M}\right]-2(A+c_1)\Delta\omega_2^2=0\end{aligned} \tag{65}$$

$$\begin{aligned}&\frac{(A+c_1)^3V}{2M}-\frac{3(A+c_1)^2Vc_1}{M}-2\left(\frac{K+C}{M}\right)c_1-\frac{3Vc_1^3}{4M}+\frac{9\omega_2^2c_1}{4}\\&c_2\left\{\frac{-3(A+c_1)^2V}{4M}-\frac{6(A+c_1)Vc_1}{M}+\frac{9Vc_1^2}{2M}-2\left[\left(\frac{K+C}{M}\right)-9\omega_2^2\right]\right\}\\&c_3\left[\frac{9(A+c_1)^2V}{2M}-\frac{3(A+c_1)^2V}{2M}+\frac{3(A+c_1)Vc_1}{M}+2\left[\left(\frac{K+C}{M}\right)-9\omega_2^2\right]\right]+18c_1\Delta\omega_2^2=0\end{aligned} \tag{66}$$

$$\frac{3(A+c_1)Vc_1^2}{2M}-\frac{3(A+c_1)^2Vc_1}{2M}+c_2\left[-\frac{3(A+c_1)^2V}{2M}+\frac{3Vc_1^2}{2M}\right]$$
$$c_3\left[-2\left(\frac{K+C}{M}\right)-\frac{3(A+c_1)^2V}{2M}-\frac{3Vc_1^2}{2M}-\frac{3(A+c_1)Vc_1}{M}+50\omega_2^2\right]=0 \tag{67}$$

Solving Eq. (65-67), we have

$$\Delta\omega_2^2=\frac{\alpha_1(\alpha_2\alpha_3-\alpha_4\alpha_5)+\alpha_6(\alpha_7\alpha_5-\alpha_2\alpha_8)+\alpha_1(\alpha_4\alpha_8-\alpha_7\alpha_3)}{\alpha_{10}(\alpha_6\alpha_8-\alpha_1\alpha_3)+\alpha_{11}(\alpha_7\alpha_3-\alpha_4\alpha_8)} \tag{68}$$

$$c_2=\frac{\alpha_{10}(\alpha_1\alpha_5-\alpha_9\alpha_8)+\alpha_{11}(\alpha_2\alpha_8-\alpha_7\alpha_8)}{\alpha_{10}(\alpha_6\alpha_8-\alpha_1\alpha_3)+\alpha_{11}(\alpha_7\alpha_3-\alpha_4\alpha_8)} \tag{69}$$

$$c_3=\frac{\alpha_{10}(\alpha_9\alpha_3-\alpha_6\alpha_5)+\alpha_{11}(\alpha_4\alpha_5-\alpha_2\alpha_3)}{\alpha_{10}(\alpha_6\alpha_8-\alpha_1\alpha_3)+\alpha_{11}(\alpha_7\alpha_3-\alpha_4\alpha_8)} \tag{70}$$

where

$$\alpha_1=\frac{3(A+c_1)^2V}{2M}-\frac{3Vc_1^2}{2M}-\frac{3(A+c_1)Vc_1}{M}$$

$$\alpha_2=\frac{(A+c_1)^3V}{2M}-\frac{3(A+c_1)^2Vc_1}{M}-2\left(\frac{K+C}{M}\right)c_1-\frac{3Vc_1^3}{4M}+\frac{9\omega_2^2c_1}{4}$$

$$\alpha_3=-\frac{3(A+c_1)^2V}{2M}+\frac{3Vc_1^2}{2M}$$

$$\alpha_4=\frac{-3(A+c_1)^2V}{4M}-\frac{6(A+c_1)Vc_1}{M}+\frac{9Vc_1^2}{2M}-2\left[\left(\frac{K+C}{M}\right)-9\omega_2^2\right]$$

$$\alpha_5=\frac{3(A+c_1)Vc_1^2}{2M}-\frac{3(A+c_1)^2Vc_1}{2M}$$

$$\alpha_6=\frac{3(A+c_1)^2V}{M}+\frac{3(A+c_1)Vc_1}{M}+2\left(\frac{K+C}{M}\right)+\frac{3(A+c_1)Vc_1^2}{M}-2\omega_2^2$$

$$\alpha_7=\frac{9(A+c_1)^2V}{2M}-\frac{3(A+c_1)^2V}{2M}+\frac{3(A+c_1)Vc_1}{M}+2\left[\left(\frac{K+C}{M}\right)-9\omega_2^2\right]$$

$$\alpha_8=\left[-2\left(\frac{K+C}{M}\right)-\frac{3(A+c_1)^2V}{2M}-\frac{3Vc_1^2}{2M}-\frac{3(A+c_1)Vc_1}{M}+50\omega_2^2\right]$$

$$\alpha_9=\frac{3(A+c_1)^3V}{2M}-\frac{3(A+c_1)^2Vc_1}{2M}-2\omega_2(A+c_1)+2\left(\frac{K+C}{M}\right)(A+c_1)+\frac{3(A+c_1)Vc_1^2}{M}$$

$$\alpha_{10}=18c_1$$

$$\alpha_{11}=-2(A+c_1)$$

It should be noted that:

$$u_3(\tau)=u_2(\tau)+\Delta u_2(\tau) \tag{71}$$

Substituting Eq. (58) and Eq. (64), we have:

$$u_3(\tau)=[A+c_1+c_2]cos(\omega_3 t)+[c_3-c_2-c_1]cos(3\omega_3 t)-c_3 cos(5\omega_3 t) \tag{72}$$

Where the third-order natural frequency is given as:

$$\omega_3=\sqrt{\left\{\left[\frac{128\left(\frac{K+C}{M}\right)^2+69A^4\left(\frac{V}{M}\right)^2+192A^2\left(\frac{K+C}{M}\right)\left(\frac{V}{M}\right)}{8\left[16\left(\frac{K+C}{M}\right)+12A^2\left(\frac{V}{M}\right)\right]}\right]+\left[\frac{\alpha_1(\alpha_2\alpha_3-\alpha_4\alpha_5)+\alpha_6(\alpha_7\alpha_5-\alpha_2\alpha_8)+\alpha_1(\alpha_4\alpha_8-\alpha_7\alpha_3)}{\alpha_{10}(\alpha_6\alpha_8-\alpha_1\alpha_3)+\alpha_{11}(\alpha_7\alpha_3-\alpha_4\alpha_8)}\right]\right\}} \tag{73}$$

Also, Eq. (69) can be written directly in terms of the primary parameters and related parameter to the primary parameters in the governing equations as:

$$
\begin{aligned}
u_3(\tau) = {} & \left\{ \left[A - \frac{A^3 V}{8M\left[4\left(\frac{K+C}{M}\right)+3A^2\left(\frac{V}{M}\right)\right]} + \frac{\alpha_{10}\left(\alpha_1\alpha_5-\alpha_9\alpha_8\right)+\alpha_{11}\left(\alpha_2\alpha_8-\alpha_7\alpha_8\right)}{\alpha_{10}\left(\alpha_6\alpha_8-\alpha_1\alpha_3\right)+\alpha_{11}\left(\alpha_7\alpha_3-\alpha_4\alpha_8\right)} \right] \times \right. \\
& \left. cos\left(\left\{ \sqrt{ \left[\frac{128\left(\frac{K+C}{M}\right)^2 + 69A^4\left(\frac{V}{M}\right)^2 + 192A^2\left(\frac{K+C}{M}\right)\left(\frac{V}{M}\right)}{8\left[16\left(\frac{K+C}{M}\right)+12A^2\left(\frac{V}{M}\right)\right]} \right] + \left[\frac{\alpha_1\left(\alpha_2\alpha_3-\alpha_4\alpha_5\right)+\alpha_6\left(\alpha_7\alpha_5-\alpha_2\alpha_8\right)+\alpha_1\left(\alpha_4\alpha_8-\alpha_7\alpha_3\right)}{\alpha_{10}\left(\alpha_6\alpha_8-\alpha_1\alpha_3\right)+\alpha_{11}\left(\alpha_7\alpha_3-\alpha_4\alpha_8\right)} \right] } \right\} t \right) \right\} \\
& + \left\{ \left[\frac{\alpha_{10}\left(\alpha_9\alpha_3-\alpha_6\alpha_5\right)+\alpha_{11}\left(\alpha_4\alpha_5-\alpha_2\alpha_3\right)}{\alpha_{10}\left(\alpha_6\alpha_8-\alpha_1\alpha_3\right)+\alpha_{11}\left(\alpha_7\alpha_3-\alpha_4\alpha_8\right)} - \frac{\alpha_{10}\left(\alpha_1\alpha_5-\alpha_9\alpha_8\right)+\alpha_{11}\left(\alpha_2\alpha_8-\alpha_7\alpha_8\right)}{\alpha_{10}\left(\alpha_6\alpha_8-\alpha_1\alpha_3\right)+\alpha_{11}\left(\alpha_7\alpha_3-\alpha_4\alpha_8\right)} + \frac{A^3 V}{8M\left[4\left(\frac{K+C}{M}\right)+3A^2\left(\frac{V}{M}\right)\right]} \right] \right. \\
& \left. \times cos\left(3\left\{ \sqrt{ \left[\frac{128\left(\frac{K+C}{M}\right)^2 + 69A^4\left(\frac{V}{M}\right)^2 + 192A^2\left(\frac{K+C}{M}\right)\left(\frac{V}{M}\right)}{8\left[16\left(\frac{K+C}{M}\right)+12A^2\left(\frac{V}{M}\right)\right]} \right] + \left[\frac{\alpha_1\left(\alpha_2\alpha_3-\alpha_4\alpha_5\right)+\alpha_6\left(\alpha_7\alpha_5-\alpha_2\alpha_8\right)+\alpha_1\left(\alpha_4\alpha_8-\alpha_7\alpha_3\right)}{\alpha_{10}\left(\alpha_6\alpha_8-\alpha_1\alpha_3\right)+\alpha_{11}\left(\alpha_7\alpha_3-\alpha_4\alpha_8\right)} \right] } \right\} t \right) \right\} \\
& - \left\{ \left(\frac{\alpha_{10}\left(\alpha_9\alpha_3-\alpha_6\alpha_5\right)+\alpha_{11}\left(\alpha_4\alpha_5-\alpha_2\alpha_3\right)}{\alpha_{10}\left(\alpha_6\alpha_8-\alpha_1\alpha_3\right)+\alpha_{11}\left(\alpha_7\alpha_3-\alpha_4\alpha_8\right)} \right) \right. \\
& \left. \times cos\left(5\left\{ \sqrt{ \left[\frac{128\left(\frac{K+C}{M}\right)^2 + 69A^4\left(\frac{V}{M}\right)^2 + 192A^2\left(\frac{K+C}{M}\right)\left(\frac{V}{M}\right)}{8\left[16\left(\frac{K+C}{M}\right)+12A^2\left(\frac{V}{M}\right)\right]} \right] + \left[\frac{\alpha_1\left(\alpha_2\alpha_3-\alpha_4\alpha_5\right)+\alpha_6\left(\alpha_7\alpha_5-\alpha_2\alpha_8\right)+\alpha_1\left(\alpha_4\alpha_8-\alpha_7\alpha_3\right)}{\alpha_{10}\left(\alpha_6\alpha_8-\alpha_1\alpha_3\right)+\alpha_{11}\left(\alpha_7\alpha_3-\alpha_4\alpha_8\right)} \right] } \right\} t \right) \right\}
\end{aligned}
\tag{74}
$$

Following the procedure given above, we write a generalized expression for the *kth*-order of analytical approximation as:

$$u_{k-1}(\tau) = \sum_{j=1}^{k-1} d_j \left\{ cos\left(2j-1\right)\tau - cos\left(2j+1\right)\tau \right\} \tag{75}$$

$$\omega_{k-1} = \sqrt{\omega_{k-2}^2 + \Delta\omega_{k-2}^2} \tag{76}$$

Also, it can easily be seen that as the nonlinear term, V tends to zero, the frequency ratio of the nonlinear frequency to the linear frequency, $\frac{\omega_3}{\omega_b}$ tends to 1:

$$\lim_{V\to 0} \frac{\omega_3}{\omega_b} = 1 \tag{77}$$

Where

$$\omega_b = \sqrt{\left[\frac{(K+C)}{M}\right]} \tag{78-a}$$

It should be pointed out that when the nonlinear term, V is set to zero, we recovered the linear natural frequency. Also, as the amplitude, A tends to zero, the frequency ratio of the nonlinear frequency to the linear frequency, $\frac{\omega_3}{\omega_b}$ tends to 1.

$$\lim_{A\to 0}\frac{\omega_3}{\omega_b}=1 \tag{78-b}$$

Furthermore, it can easily be shown that

$$\lim_{t\to 0}u_3(t)=A \tag{79}$$

And for very large values of the amplitude A, we have

$$\lim_{A\to \infty}\frac{\omega}{\omega_b}=\infty \tag{80}$$

Where *M, K, C and V are respective integral values of the respective space functions of the respective boundary conditions and structure considered.* On a general note, following Lai *et al.* [67], it can easily be shown that the exact natural frequency of the fluid-conveying structures is given as:

$$\omega_{1,exact}=\frac{\pi\xi_1}{2\left[\int_0^{\pi/2}\left(1-\xi_2^2 sin^2 t\right)^{-\frac{1}{2}}dt\right]} \tag{81-a}$$

For the general case in this work,

$$\xi_1=\sqrt{\left[\left(\frac{K+C}{M}\right)-\left(\frac{VA^2}{2M}\right)\right]}\qquad \xi_2=\sqrt{\frac{\frac{VA^2}{2M}}{\left[\frac{(K+C)}{M}-\frac{VA^2}{2M}\right]}} \tag{81-b}$$

Where when the nonlinear term, V is set to zero, we recovered the linear natural frequency. Although, it is very difficult to generate a general exact solution of Eq. (78). However, on using series integration method, we developed an analytical solution for the nonlinear natural frequency as:

$$\omega_{exact}=\frac{\xi_1}{1+\left(\left(\frac{1}{2}\right)^2\xi_2^2+\left(\frac{1}{2}\cdot\frac{3}{4}\right)^2\xi_2^4+\left(\frac{1}{2}\cdot\frac{3}{4}\cdot\frac{5}{6}\right)^2\xi_2^6+\left(\frac{1}{2}\cdot\frac{3}{4}\cdot\frac{5}{6}\cdot\frac{7}{8}\right)^2\xi_2^8+\ldots+\left(\prod_{n=1}^{N}\frac{2n-1}{2n}\right)^2\xi_2^{2N}\right)} \tag{82}$$

We also developed an approximated analytical solution:

$$\omega_{approx.}=\frac{\xi_1}{\left(1+0.25000\xi_2+0.11680\xi_2^{\,2}+0.59601\xi_2^{\,3}-1.90478\xi_2^{\,4}+2.04574\xi_2^{\,5}\right)} \tag{83}$$

It can easily be seen that as the nonlinear term tends to zero, the frequency ratio of the approximated nonlinear frequency to the exact nonlinear frequency, $\frac{\omega_3}{\omega_{exact}}$ tends to 1.

$$\lim_{V\to 0}\frac{\omega_3}{\omega_{exact}}=1 \tag{84}$$

Also, it could be observed that as the amplitude A tends to zero, the frequency ratio of the approximated nonlinear frequency to the exact nonlinear frequency, $\frac{\omega_3}{\omega_{exact}}$ tends to 1.

$$\lim_{A\to 0}\frac{\omega_3}{\omega_{exact}}=1 \tag{85}$$

6. Results and Discussion

The first five normalized mode shapes of the beams for clamped-clamped, simple-simple, clamped-simple and clamped-free supports are shown in Fig. 2-5. Also, the figures show the deflections of the beams along the beams' span at five different buckled and mode shapes.

Figs. 6-9 show the comparison of hyperbolic-trigonometric and the polynomial functions for the normalized mode shapes of the beams for clamped-clamped, simple-simple, clamped-simple and clamped-free supports. The figures depict the validity of the developed polynomial functions in this work as there are very good agreements between the hyperbolic-trigonometric and the developed polynomial functions.

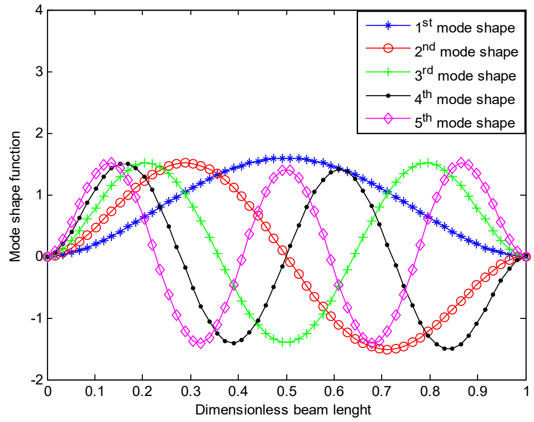

Fig. 2. The first five normalized mode shaped of the beams under clamped-clamped supports

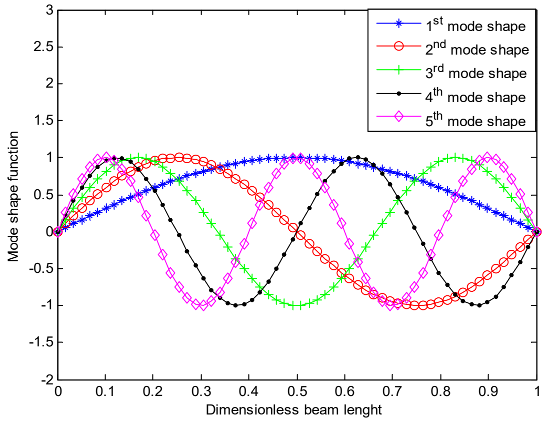

Fig. 3. The first five normalized mode shaped of the beams under simple-simple supports

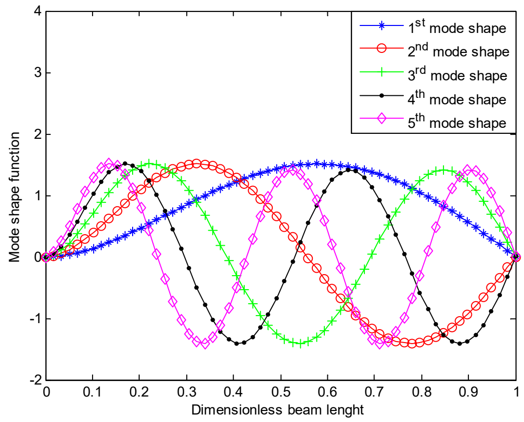

Fig. 4. The first five normalized mode shaped of the beams under clamped-simple supports

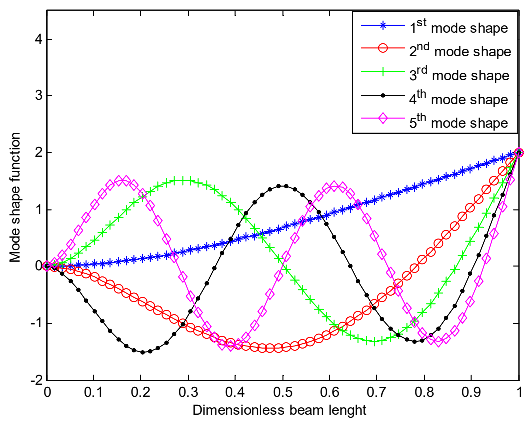

Fig. 5. The first five normalized mode shaped of the beams under clamped-free (cantilever) supports

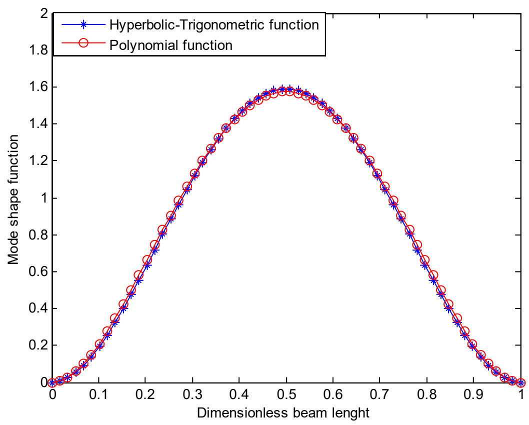

Fig. 6. Normalized mode shaped of the structures under clamped-clamped supports for Hyperbolic-Trigonometric and Polynomial functions

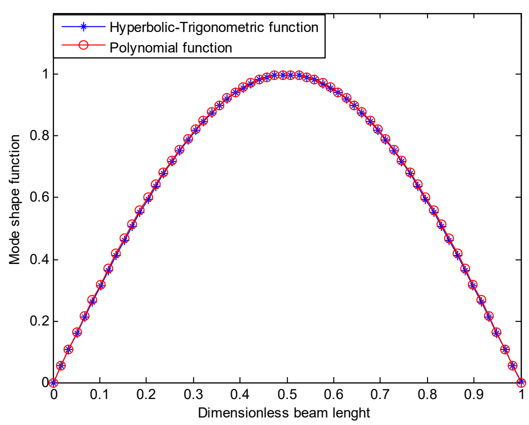

Fig. 7. Normalized mode shaped of the structures under simple-simple supports for Hyperbolic-Trigonometric and Polynomial functions

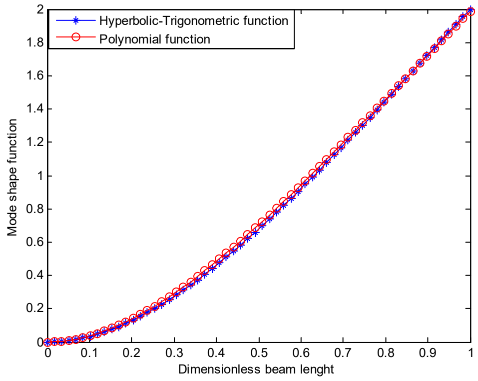

Fig. 8. Normalized mode shaped of the structures under clamped-free supports for Hyperbolic-Trigonometric and Polynomial functions

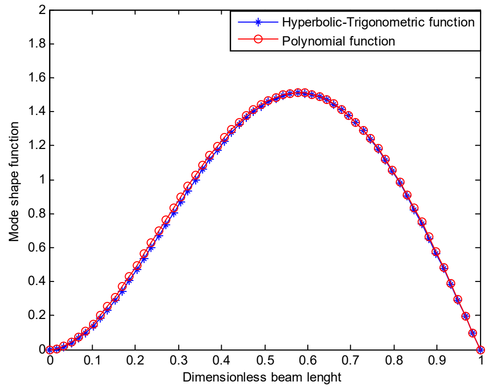

Fig. 9. Normalized mode shaped of the structures under clamped-simple supports for Hyperbolic-Trigonometric and Polynomial functions

Fig. 10 illustrates the effects of boundary conditions on the nonlinear amplitude-frequency response curves of the nanotube. Also, the figure shows the variation of frequency ratio of the nanotube with the dimensionless maximum amplitude of the structure under different boundary conditions. From, the result, it shown that frequency ratio is highest in the beam which is clamped-free (cantilever) supported beam and lowest with clamped-clamped beam. The lowest frequency ratio of the clamped-clamped beam is due to high stiffness of the beam with this type of boundary conditions in comparison with other types of boundary conditions. The fundamental linear vibration frequency is the lowest root of the resulting characteristics equation. It can be seen from the figure, in contrast to linear systems, the nonlinear frequency is a function of amplitude so that the larger the amplitude, the more pronounced the discrepancy between the linear and the nonlinear frequencies becomes.

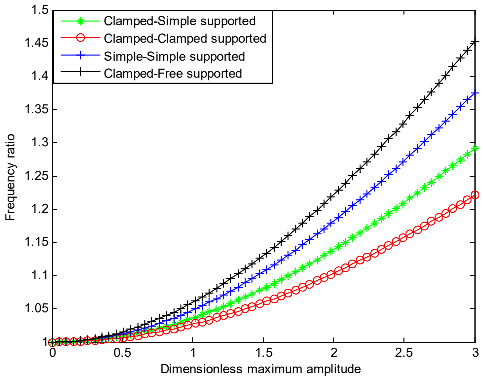

Fig. 10. Effects of boundary conditions on the nonlinear amplitude-frequency response curves of the nanotube

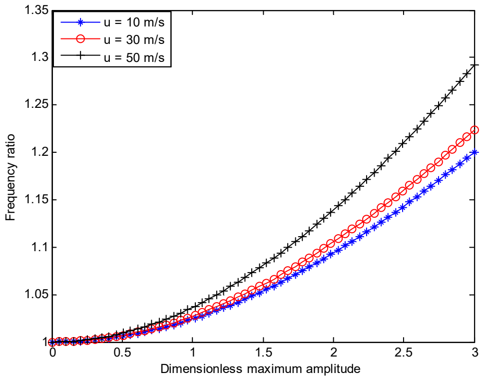

Fig. 11. Effects of fluid-flow velocity on the nonlinear amplitude-frequency response curves of CNT

Fig. 11 shows effects of fluid-flow velocity on the nonlinear amplitude-frequency response curves of pipe. It is observed that with increase of the length or by extension, the aspect ratio of the pipe, the nonlinear vibration frequencies of the structure decreases while nonlinear vibration frequencies increases with the increase in the fluid-flow velocity.

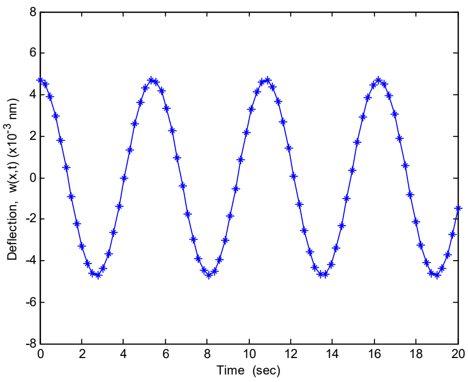

Fig. 12. Midpoint deflection time history for the nonlinear analysis of SWCBT when Kn=0.03 and U= 100 m/s

Fig. 12 illustrates the midpoint deflection time history for the nonlinear analysis of SWCBT when *Kn = 0.03* and *U= 100 m/s* while Fig. 13 presents the midpoint deflection time history for the nonlinear analysis of SWCBT when *Kn = 0.03* and *U= 500 m/s*. Also, Fig. 14 depicts the midpoint deflection time history for the linear analysis of SWCBT when *Kn = 0.03* and *U= 500 m/s.* Comparing Fig. 13 and 14,the stretching effects on the dynamic behaviours of the SWCNT is depicted. It is depicted that increase in the slip parameter leads to decrease in the frequency of vibration and by extension, decrease in the critical velocity.

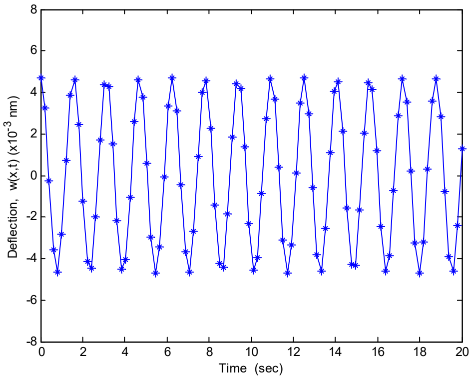

Fig. 13. Midpoint deflection time history for the nonlinear analysis of SWCBT when Kn=0.03 and U= 500 m/s

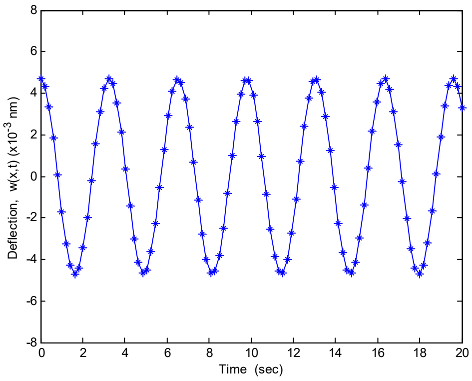

Fig. 14. Midpoint deflection time history for the linear analysis of SWCBT when Kn=0.03 and U= 500 m/s

Fig. 15 shows the comparison of the linear vibration with nonlinear vibration of the SWCNT. It could be seen in the figure that the discrepancy between the linear and nonlinear amplitudes increases with increment of the maximum vibration. The nonlinear effects show the stretching effects. As stretching effect increases, the stiffness of the system increases which consequently, increases in the natural frequency and the critical fluid velocity.

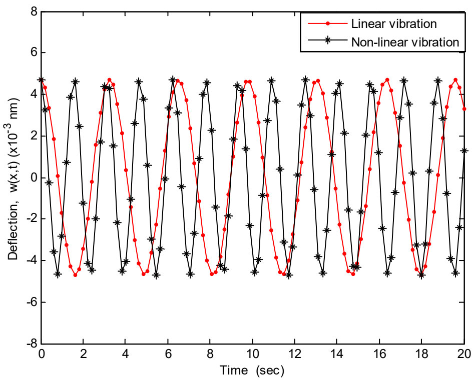

Fig. 15. Comparison of midpoint deflection time history for the linear and nonlinear analysis of CBT when Kn=0.03 and U= 500 m/s

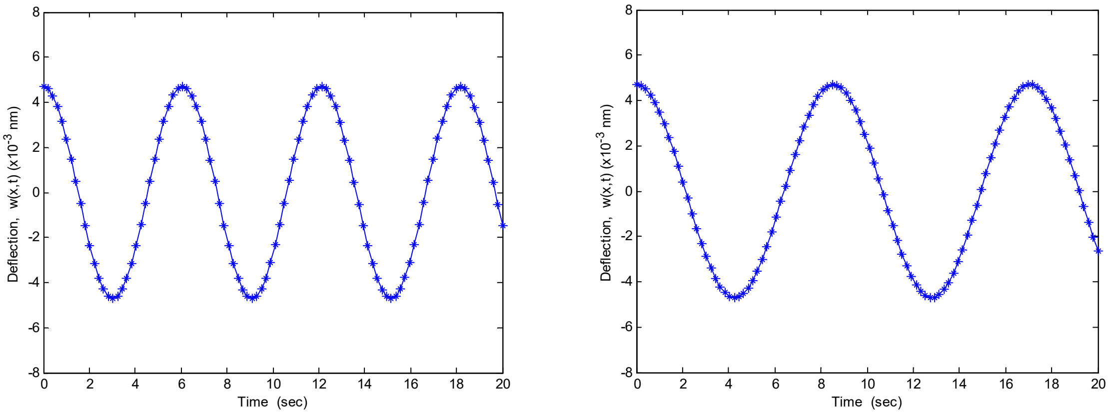

Fig. 16. Effects of slip parameter on the deflection of the nonlinear vibration (a) Kn=0.03 (b) Kn = 0.05

Effects of slip parameter, Knudsen number on the vibration of the nanotube is shown in Fig.16. It is depicted that increase in the slip parameter leads to decrease in the frequency of vibration and by extension, decrease in the critical velocity.

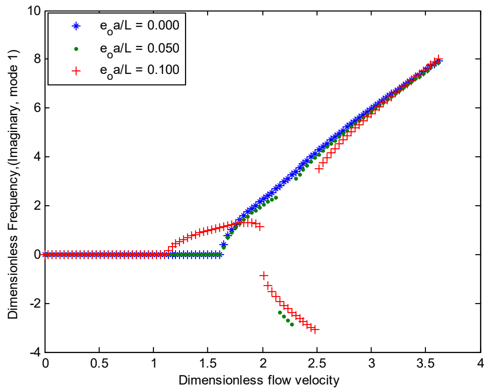

(a)

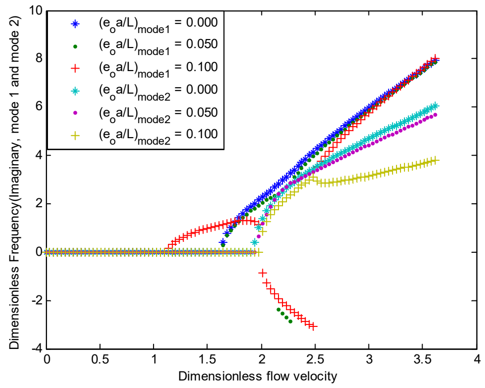

(b)

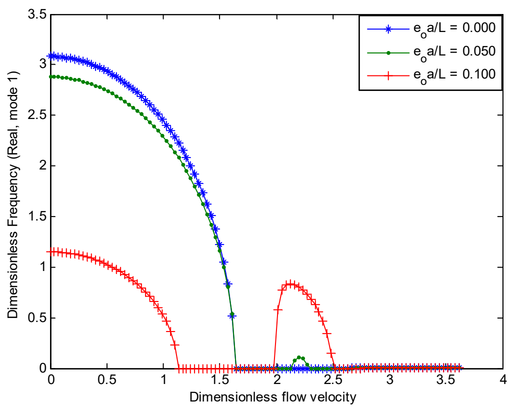

(c)

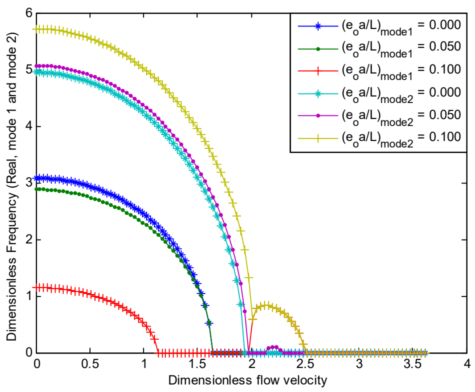

(d)

Fig. 17. a-d Effects of nonlocal parameter and fluid flow velocity on the natural frequency of the nonlinear vibration

In order to investigate the vibrational and stability behaviors of the structure, effects of fluid flow velocity on the natural frequencies are carried out. As the flow velocity is increased from zero, the nanotube becomes more flexible and the fundamental frequencies decreases as shown in Fig. 17 a-d. The natural frequency becomes zero when the flow velocity of the conveyed fluid exceeds a certain value which corresponds to the critical flow velocity. Also, the Figures depict the critical speeds corresponding to the divergence condition for different values of the system's parameters. It should be pointed out that as the total mass of the system which comprised of the masses of fluid and CNT increases, the frequency of vibration decreases. When the system becomes stiffer (the stiffness of the system due to bending and shears rigidities whose values depend on the second moment of inertia and the cross-sectional areas of the CNC and the fluid), the nanotube vibrates at higher frequencies. For a CNT with certain characteristics, the term, m_fU^2 is constant along the nanotube's length and the system's flexibility decreases as the flow velocity becomes greater. The real and imaginary parts of the eigenvalues related to the two lowest modes with different nanotube parameters are plotted for a range of dimensionless velocity, 0 - 4. It is found that the frequency of the first mode becomes zero in vicinity of dimensionless velocity 1.18 while for the second mode, in the vicinity of 2.0. When the flow velocity reaches the critical velocity, both the real and imaginary parts of the flexural frequency are equal to zero for the first mode, which corresponds to a point of bounded neutral stability. When the velocity of the fluid is greater than the critical velocity, the vibration frequency is zero. Although, the effect of the nonlocal parameter on flexural frequency is not very significant, it is considered in this study because the small scale can affect the critical flow velocity, as shown in Fig. 17. It could be inferred that by increasing the nonlocal parameter, the natural frequency and the critical velocity decreased. Fig. 18a-b shows the effects of temperature change on the frequencies of the CNT. From the figure, as the temperature change increases, the natural frequencies and the critical flow velocity of the structure increase.

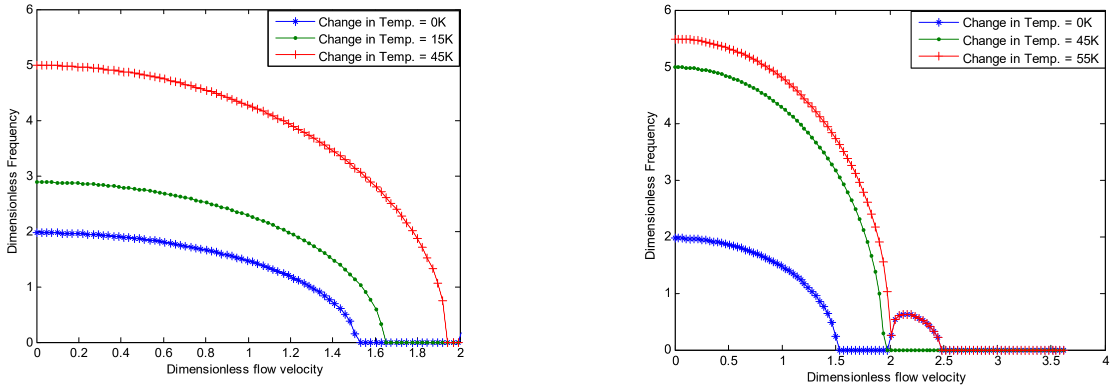

(a) (b)

Fig. 18. a-b Effects of temperature and fluid flow velocity on the natural frequency of the nonlinear vibration at low/room temperature

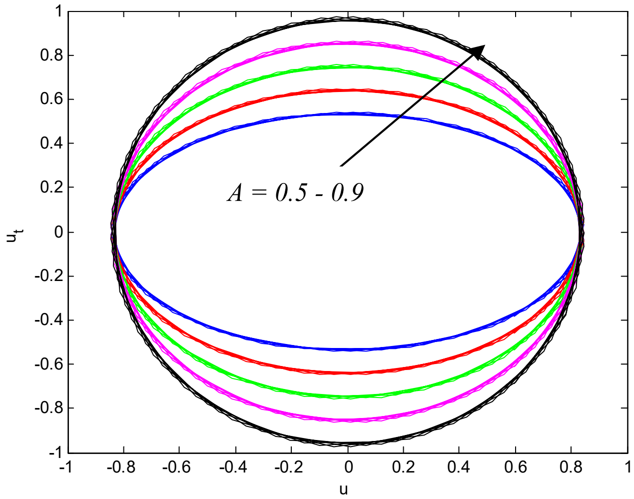

Fig. 19. Phase-space curve of u_t versus u

Fig. 19 shows a phase-space/plane curve of u_t versus u which shows the behaviour of the oscillator. The phase plots show the behaviour of the oscillator when the amplitude is varied. It is periodic with center (0, 0) where stability conditions can be observed. This situation is common in unforced, undamped cubic Duffing oscillators.

7. Conclusion

In this paper, unified analytical solutions are developed for the nonlinear equations arising in flow-induced vibrations through pipes, micro-pipes and nanotubes using Galerkin-Newton-Balancing Method (GNBM). The results showed that the alteration of nonlinear flow-induced frequency from linear frequency is tied to increasing amplitude of oscillations, flow velocity, and thermal parameters. It can be concluded that as a starting point for understanding the relationship between the physical quantities in these problems, the developed analytical solutions can provide continuous physical insights into the problems than pure numerical or computational methods and can also serve as a methodto verify the numerical or approximate analytical solutions.

References

[1] Iijima, S. Nature, London, Vol. 354, pp. 56(1991), 56–58.
[2] Benjamin. T. B. Dynamics of a system of articulated pipes conveying fluid. I. Theory. Proc R Soc A Vol. 261:pp. 487–99, 1961.
[3] Holmes, P. J. Pipe Supported at Both Ends cannot Flutter. Journal of Applied Mechanics. Vol. 45, pp. 669-672, 1978
[4] Housner, G. W., Dodds, H. L. and Runyan. H. Effect of High Velocity Fluid Flow in the Bending Vibration and Static Divergence of Simply Supported Pipes. National Aeronautics and Space Administration Report NASA TN D- 2870, June 1965.
[5] Naguleswaran, S. and Williams, C. J. H., Lateral Vibration of a Pipe Conveying Fluid. Journal of Mechanical Engineering Science.Vol. 10, pp. 228- 238, 1968.
[6] Paidoussis, M. P., Dynamics of Flexible Slender Cylinders in Axial Flow. Journal of Fluid Mechanics. Vol. 26, pp. 717-736, 1966
[7] Paidoussis, M. P. and Deksnis, E. B. Articulated Models of Cantilevers Conveying Fluid: the Study of Paradox. The Journal of Mechanical Engineering Science. Vol. 12, pp. 288-300, 1970.
[8] Paidoussis, M. P. and Issid, T. D. Dynamics Stability of Pipes Conveying Fluid. Journal of Sound and Vibration. Vol. 33, pp. 267-294, 1974.
[9] Paidoussis, M. P. and Laither, T. D. Dynamics of Timoshenko Beam Conveying Fluid. Journal of Mechanical Engineering Science, Vol. 18, pp. 210-220, 1976.
[10] Paidoussis, M. P., Luu, T. R. and Laither, B. E. Dynamics of Finite Length Tubular Beams Conveying Fluid. Journal of Sound and Vibration. Vol. 106 (2), pp. 311-331, 1986.
[11] Paidoussis, M. P. Fluid-structure interactions: slender structures and axial flow, vol. 1. London: Academic Press; 1998.
[12] Semler., C., Li, G. X. and Paidoussis, M. P. The Non-Linear Equations of Motion of Pipes Conveying Fluid. Journal of Sound and Vibration, Vol. 169, 577-599, 1999.
[13] Rinaldi, S., Prabhakar, S., Vengallatore, S. Paıdoussis, M. P. Dynamics of microscale pipes containing internal fluid flow: damping, frequency shift, and stability. J Sound Vib. Vol. 329, pp.1081–1088., 2010
[14] Akgoz, B. and Civalek, O. Free vibration analysis of axially functionally graded tapered Bernoulli–Euler microbeams based on the modified couple stress theory. Compos. Struct., Vol. 98, pp. 314–22, 2013
[15] Wang L. Size-dependent vibration characteristics of fluid-conveying microtubes. J Fluid Struct. Vol. 26 pp. 675–84, 2010.
[16] Xia, W. and Wang, L. Microfluid-induced vibration and stability of structures modeled as microscale pipes conveying fluid based on non-classical Timoshenko beam theory. Microfluid Nanofluid Vol. 9, pp. 955–62, 2010.
[17] Ahangar, S., Rezazadeh, G., Shabani, R., Ahmadi, G., Toloei, A. On the stability of a microbeam conveying fluid considering modified couple stress theory. Int. Journal Mech. Vol. 7, 327–42, 2011.
[18] Yin, L., Qian, Q. Wang. L. Strain gradient beam model for dynamics of microscale pipes conveying fluid. Appl Math Model. Vol. 35, pp. 2864–73, 2011.
[19] Sahmani, S. Bahrami, M, Ansari. R. Nonlinear free vibration analysis of functionally graded third-order shear deformable microbeams based on the modified strain gradient elasticity theory. Compos Struct. Vol. 110, pp. 219–30, 2014.
[20] Akgoz, B. and Civalek, O. Buckling analysis of functionally graded microbeams based on the strain gradient theory. Acta Mech. Vol. 224, pp. 2185–201, 2013.
[21] Zhao, J., Zhou, S. Wang, B. Wang, X. Nonlinear microbeam model based on strain gradient theory. Appl Math Model. Vol. 36, 2674–86, 2012.
[22] Akgoz, B. and Civalek, O. Shear deformation beam models for functionally graded microbeams with new shear correction factors. Compos Struct. Vol.112: pp. 214–25, 2014.
[23] Kong, S. L. Zhou, S. J. , Nie,Z. K., Wang, K. Static and dynamic analysis of micro beams based on strain gradient elasticity theory. Int J Eng Sci. Vol. 47, pp. 487–98, 2009.
[24] Asghari, M., Ahmadian, M., Kahrobaiyan, M., Rahaeifard, M. On the size-dependent behavior of functionally graded micro-beams. Mater Des. Vol. 31, pp. 2324–2329, 2010.
[25] Yang, T. Z., Ji, S., Yang, X. D., Fang, B. Microfluid-induced nonlinear free vibration of microtubes. Int J Eng Sci. Vol. 76, pp. 47–55, 2014.
[26] Ke, L.L. Wang, Y.S. Yang, J., Kitipornchai, S. Nonlinear free vibration of size dependent functionally graded microbeams. Int J Eng Sci. Vol. 50, pp. 256–67, 2010.
[27] Salamat-Talab, M., Shahabi, F., Assadi, A. Size dependent analysis of functionally graded microbeams using strain gradient elasticity incorporated with surface energy. Appl Math Model Vol. 37, pp. 507–26, 2013.
[28] Setoodeh, R., Afrahhim, S. Nonlinear dynamic analysis of FG micro-pipes conveying fluid based on strain gradient theory. Composite Structures, Vol. 116, pp. 128-135, 2014.
[29] Yoon, G., Ru,C. Q. and Mioduchowski, A. Vibration and instability of carbon nanotubes conveying fluid, Journal of Applied Mechanics, Transactions of the ASME, Vol. 65(9), pp. 1326–1336, 2005.
[30] Y.an, Y. Wang, W. Q. Zhang, L. X. Nonlocal effect on axially compressed buckling of triple-walled carbon nanotubes under temperature field, Journal of Applied Math and Modelling, Vol. 34, pp. 3422–3429, 2010
[31] Murmu, T. and Pradhan, S.C. Thermo-mechanical vibration of Single-walled carbon nanotube embedded in an elastic medium based on nonlocal elasticity theory, Computational Material Science, Vol. 46 , pp. 854–859, 2009.
[32] Yang, H. K. Wang, X. Bending stability of multi-wall carbon nanotubes embedded in an elastic medium, Modeling and Simulation in Materials Sciences and Engineering, Vol. 14, 99, 99–116, 2006.
[33] Yoon, J., Ru, C. Q., Mioduchowski, A. Vibration of an embedded multiwall carbon nanotube, Composites Science and Technology, Vol. 63(11) , pp. 1533–1542, 2003.
[34] Chang, W. J. and Lee, H. L. Free vibration of a single-walled carbon nanotube containing a fluid flow using the Timoshenko beam model, Physics Letter A, Vol. 373 (10), pp. 982–985, 2009.
[35] Lu, P., Lee, H. P., Lu, C., Zhang, P. Q. Application of nonlocal beam models for carbon nanotubes, International Journal of Solids and Structures, Vol. 44(16), pp.5289–5300, 2007.
[36] Zhang, Y., Liu, G., Han, X. Transverse vibration of double-walled carbon nanotubes under compressive axial load, Applied Physics Letter A, Vol. 340 (1-4), pp. 258–266, 2005.
[37] Arani, G., Zarei, M. S., Mohammadimehr, M., Arefmanesh, A., Mozdianfard, M. R. The thermal effect on buckling analysis of a DWCNT embedded on the Pasternak foundation, Physica E, Vol. 43, pp. 1642–1648, 2011.

[38] Sobamowo, M. G. Thermal analysis of longitudinal fin with temperature-dependent properties and internal heat generation using Galerkin's method of weighted residual. Applied Thermal Engineering, Vol. 99 pp. 1316–1330, 2016
[39] Zhou, J. K. Differential Transformation and its Applications for Electrical Circuits. *Huazhong University Press: Wuhan, China* (1986)
[40] Ho, S. H. and Chen, C. K. Analysis of general elastically end restrained non-uniform beams using differential transform. *Appl. Math. Modell.* Vol. 22, pp. 219-234, 1998.
[41] Chen, C. K. and Ho, S. H. Transverse vibration of a rotating twisted Timoshenko beams under axial loading using differential transform. *Int. J. Mechanical Sciences*. Vol. 41, pp. 1339-1356, 1999.
[42] Chen, C. K. and Ho., S. H. Application of Differential Transformation to Eigenvalue Problems. Journal of Applied Mathematics and Computation, Vol. 79, pp. 173-188, 1996.
[43] Cansu, Ü. and Özkan, O. Differential Transform Solution of Some Linear Wave Equations with Mixed Nonlinear Boundary Conditions and its Blow up. Applied Mathematical Sciences Journal, Vol. 4(10), 467-475, 2010.
[44] Chang, S. H. and Chang. I. L. A New Algorithm for Calculating Two-dimensional Differential Transform of Nonlinear Functions. Journal of Applied Mathematics and Computation, Vol. 215, pp. 2486-2494, 2009.
[45] Chen, C. L. and Liu, Y. C. Two-dimensional Differential Transform for Partial Differential Equations. Journal of Applied Mathematics and Computation. Vol. 121, pp. 261-270, 2001.
[46] Jafari, H., M., Alipour, H. M. and H. Tajadodi. Two-dimensional Differential Transform Method for Solving Nonlinear Partial Differential Equations. International Journal of Research and Reviews in Applied Sciences, Vol. 2(1), pp. 47-52, 2010.
[47] Kaya, M. O. Free Vibration Analysis of a Rotating Timoshenko Beam by Differential Transform Method. Aircraft Engineering and Aerospace Technology Journal, Vol. 78(3), pp. 194-203, 2006.
[48] Jang, M. J., Chen, C. L. Liy, Y. C. On solving the initial-value problems using the differential transformation method. Appl. Math. Comput. Vol. 115, pp. 145-160, 2000.
[49] K¨oksal, M., and Herdem, S. Analysis of nonlinear circuits by using differential Taylor transform. *Computers and Electrical Engineering*. Vol. 28, pp.513-525, 2008.
[50] Hassan, I. H. A. H. Different applications for the differential transformation in the differential equations. Appl. Math. Comput. Vol. 129, pp. 183-201, 2002.
[51] Ravi, A. S. V. Kanth, K. Aruna: Solution of singular two-point boundary value problems using differential transformation method. *Phys. Lett. A*. Vol. 372, pp. 4671-4673, 2008.
[52] Chen, C. K. and Ho S.H. Solving partial differential equations by two-dimensional differential transform method. Appl. Math. Comput. Vol. 41, pp. 171-179, 1999.
[53] Ayaz, F. On two-dimensional differential transform method. *Appl. Math. Comput.Vol.* 143, pp. 361-374, 2003.
[54] Ayaz, F. Solutions of the system of differential equations by differential transform method. *Appl. Math. Comput.*147: pp. 547-567, 2004.
[55] Chang, S. H. and Chang, I.L., A new algorithm for calculating one-dimensional differential transform of nonlinear functions. *Appl. Math. Comput. Vol.* 195, pp. 799-808, 2008.
[56] Momani, S. and Ert¨urk, V. S. Solutions of non-linear oscillators by the modified differential transform method. *Computers and Mathematics with Applications*. Vol. 55(4), 833-842, 2008.
[57] Momani, S., 2004. Analytical approximate solutions of non-linear oscillators by the modified decomposition method. Int. J. Modern. Phys. C, Vol. 15(7), pp. 967-979, 2004.
[58] El-Shahed, M. Application of differential transform method to non-linear oscillatory systems. *Communic.Nonlin.Scien.Numer.Simul. Vol.* 13, pp. 1714-1720, 2008.
[59] Venkatarangan, S. N., Rajakshmi, K. A modification of adomian's solution for nonlinear oscillatory systems. *Comput.Math. Appl. Vol.* 29, pp. 67-73, 1995.
[60] Jiao, Y. C. Yamamoto, Y. C. Dang, C. Hao, C. An aftertreatment technique for improving the accuracy of Adomian's decomposition method. *Comput.Math. Appl. Vol.* 43, pp. 783-798, 2002.
[61] Elhalim, A. and Emad, E. A new aftertratment technique for differential transformation method and its application to non-linear oscillatory system. Internation Journal of Non-linear Science, Vol. 8(4), pp. 488-497, 2009.
[62] Lai, S. K., Lim, C. W., Wu, B. S. Newton-harminic balancing approach for accurate solutions to nonlinear cubic-quintic Duffing oscillators.Applied Math.Modeling, Vol. 33, pp. 852-866, 2009.
[63] Eringen, A. C. On differential equations of nonlocal elasticity and solutions of screw dislocation and surface waves, Journal of Applied Physics, Vol. 54 (9), pp. 4703–4710, 1983.
[64] Eringen, A. C. Linear theory of nonlocal elasticity and dispersion of plane waves, Inter- national Journal of Engineering Science, Vol. 10 (5), pp. 425–435, 1972.
[65] Eringen, A. C and D.G., B. Edelen, D. G. B. On nonlocal elasticity, International Journal of Engineering Science, Vol. 10 (3), pp. 233–248, 1972.
[66] Eringen, A. C. Nonlocal continuum field theories, Springer, New York 2002.
[67] Shokouhmand, H., Isfahani A. H. M. and Shirani, E. Friction and heat transfer coefficient in micro and nano channels with porous media for wide range of Knudsen number, International Communication in Heat and Mass Transfer, Vol. 37, pp. 890-894, 2010.